Torsional creep of

Alloy 617 tubes at high temperature

H.J. Penkalla, F. Schubert, H. Nickel

Nuclear Research Centre, KFA-Jülich
Institute for Reactor Materials,
P.O. Box 19 13, 5170 Jülich, Germany

Abstract:
The multiaxial creep of Alloy 617 tubes at temperatures above 900 °C is evaluated by theoretical calculations and by experimental tests with the main emphasis to torsion loading. The stress-strain-time behaviour can be discribed satisfactorally by the v. Mises theory and the use of Norton's typ creep law.

I. Introduction

With the increase of application temperatures for components in power plants up to 1000 °C the main concern for the design and analysis of the component behaviour is the time dependent materials behaviour. To describe the stress-strain-time relationship data from uniaxial creep tests are used. From these test results structural design values such as creep strain limits and creep rupture strength are derived. The mathematical description of the strain-time behaviour is based on experimentally obtained creep curves. The inelastic analysis of the component gives the base for the evaluation of component behaviour under complex loading conditions. The mathematical description of the strain-time relationship, obtained from the uniaxial test, is transfered to a three-dimensional formulation /1/. The aim of this presentation is to investigate and verify or modify the above mentioned formalism for multiaxial creep.

2. Principles

The investigation of creep in tubes is part of a general evaluation programme of materials development for high temperature components of an intermediate heat exchanger (IHX) in a nuclear process heat plant. The loading conditions for the test reflect mainly upset and emergency conditions. For the theoretical description of multiaxial creep the theory of invariances, in which the v. Mises hypothesis and the Norton's creep law are integrated, is applied.

2.1 Test pieces

The present candidates for the high temperature components in a nuclear

Superalloys 1988
Edited by S. Reichman, D.N. Duhl,
G. Maurer, S. Antolovich and C. Lund
The Metallurgical Society, 1988

process heat plant are Alloy 800 (X10NiCrAlTi 32 20) and Alloy 617 (NiCr22Co12Mo). Alloy 617 is a commonly used material for combustion chambers, hot ducting and piping in gas turbines as well as for tubing of heat exchanging components and shows the highest creep rupture strength of the two candidates.

tube dimensions		spec. form (tube test)
IHX – tube:	22 x 2.2 mm	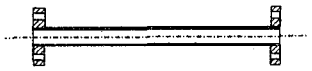
reformer tube:	120 x 10 mm	
buckling test:	40 x 3,5 mm	

mean chemical composition (wt–%)									
alloy	Fe	Ni	Cr	Al	Ti	Mn	Co	Mo	C
Alloy 800	bal.	32	22	0.4	0.4	1.0	–	–	0.06
Alloy 617	–	bal.	22	0.9	0.4	0.2	12	9	0.06

Table 1: Table of specimens form and investigated materials.

2.2 Loading and temperature ranges and material behaviour

The material behaviour under mechanical loading is principally divided into elastic, plastic (time independent), creep (time dependent). Fig. 1 shows schematically the separation of the material behaviour dependent on the loading and temperature. The different ranges overlap partly. The loading conditions discussed here lead to a time dependent creep, so only the range III must be considered.

An analysis of the operation and emergency conditions of heat exchanging components provides the following conditions: temperature 900 °C; stress intensity 30 MPA; strain rates 3×10^{-2} % min^{-1}. Fig. 2 shows the stationary creep rate as a function of stress, obtained in the uniaxial creep tests, and illustrates the range of the considered loading condition.

2.3 Uniaxial creep

A scatterband evaluation of test results from more than 300 creep tests showed that Norton's creep law (power law creep) /3/ is a good fit to describe the stationary creep. Fig. 2 shows this result for one melt. In Norton's creep law the stationary creep rate $\dot{\varepsilon}$ is a function of σ as follows

$$\dot{\varepsilon} = k'(\sigma/E)^n = k\,\sigma^n \text{ with E as Youngs Modulus.} \qquad (1)$$

2.4 Multiaxial creep

The transfer of the uniaxial creep law to multiaxial exposure leads to a static indefinite problem. The solution of this problem requires additional postulates and a materials law. For the further considerations, the following postulates are important:

- Constancy of volume:
  This is equivalent with the application of the stress deviator for the calculation of the deformation
- Compatibility:
  This means the continuity of the strain rate distribution
- Invariance of coordinates:
  The result of the calculation must be independent of the selection of coordinates
- No hardening rules:
  There should be always an equilibrium between strain rate and the true stresses in the component

- Isotropy:
  The materials behaviour is the same in all dimensions of the component
- Materials law:
  For stationary creep Norton's creep law is assumed to apply.

For a given loading σ_{ij} is the stess tensor and σ^*_{ij} the related deviator. Reflecting the assumed postulate and using Norton's creep law, the tensor of stationary creep rate is given by

$$\dot{\varepsilon}_{ij} = \frac{3}{2} k \sigma_v^{n-1} \cdot \sigma_{ij}^* \qquad (2)$$

with σ_v as the deviatoric stress according the v. Mises hypothesis. The tube geometry suggests cylindrical coordinates, therefor, the compatibility leads to

$$\frac{d\,\sigma_r}{d\,r} = \frac{1}{r} (\sigma_u - \sigma_r) \qquad (3)$$

with σ_r as radial stress component, σ_u the circumferential stress component and r the radius. In thin walled tubes, the stress distribution across the wall can be replaced by membrane stresses, so that the calculation is static definite without the application of compatibility /4, 5, 6/.

Under additional estimation of the elastic strain proportion, the complete description of multiaxial strain rate follow the equation:

$$\dot{\varepsilon}_{ij} = \frac{1+\nu}{E} \dot{\sigma}^*_{ij} + \frac{1-2\nu}{E} S \cdot \delta_{ij} + \frac{3}{2} k \sigma_v^{n-1} \sigma^*_{ij} \qquad (4)$$

with ν as Poisson's ratio, S the trace of the stress tensor, δ_{ij} the Kronecker symbol.

2.5 Discussion of typical tube loadings

In power plants tubes are stressed by primary loads such as internal pressure, tension, bending and torsion. Except for the shear stresses caused by a torque all stresses are directed in the cylindrical main axis of the tube; therefore, an analytical description is possible and quite simple. Secondary stresses due to temperature transients are mostly in the axial direction. In helix tubes, e.g. in helix heat exchanger component, secondary stresses can be torsional shear stresses.

The simplest case of loading is the unique tensile stress in axial direction. The result of the calculation is identical with the normal creep curve. The stress tensor and stress deviator are

$$\sigma_{ij} = \begin{pmatrix} 0 & 0 & 0 \\ 0 & 0 & 0 \\ 0 & 0 & \sigma \end{pmatrix} \quad \text{and} \quad \sigma^*_{ij} = \begin{pmatrix} -1/3\sigma & 0 & 0 \\ 0 & -1/3\sigma & 0 \\ 0 & 0 & 2/3\sigma \end{pmatrix} \qquad (5)$$

and the deviatoric stress is given by $\sigma_v = \sigma$.

The strain rates are:

$$\dot{\varepsilon}_z = k \sigma^n; \quad \dot{\varepsilon}_r = \dot{\varepsilon}_u = -1/2 k \sigma^n \qquad (6)$$

For tubes under internal pressure p the stress tensor and deviator is given by

$$\sigma_{ij} = \begin{pmatrix} \sigma_r & 0 & 0 \\ 0 & \sigma_u & 0 \\ 0 & 0 & \sigma_z \end{pmatrix} \quad \text{and} \quad \sigma^*_{ij} = \begin{pmatrix} \sigma_r - 1/3\,S & 0 & 0 \\ 0 & \sigma_u - 1/3\,S & 0 \\ 0 & 0 & \sigma_z - 1/3\,S \end{pmatrix} \qquad (7)$$

with $\sigma_r = 0$, $\sigma_u = \Delta pr/d$, $\sigma_z = 1/2 \Delta pr/d$, $S = \sigma_r + \sigma_u + \sigma_z$ and $\sigma_v = \sqrt{3}/2 \quad \Delta p\ r/d$

Under unique internal pressure tubes show no axial strain rate, this means the plane strain condition. This leads to the strain rates:
$\dot{\varepsilon}_z = 0$; and $\dot{\varepsilon}_u = -\dot{\varepsilon}_r = (\sqrt{3}/2)^{n+1} k (\Delta pr/d)^n$ (8)

The loading of a tube by a torque represents a plane stress condition. The stress tensor and the deviator are indentically is given by

$$\sigma_{ij} = \sigma^*_{ij} = \begin{pmatrix} 0 & 0 & 0 \\ 0 & 0 & \tau \\ 0 & \tau & 0 \end{pmatrix} \quad (9)$$

The shear stresses are eigenvalues of the tensor and provide after principle axis transformation the tensor

$$\sigma^t_{ij} = \begin{pmatrix} 0 & 0 & 0 \\ 0 & -\tau & 0 \\ 0 & 0 & \tau \end{pmatrix} \quad (10)$$

The deviatoric stress is then give by $\sigma_v = \sqrt{3}\,\tau$, and the calculated strain rates are:

$$\dot{\varepsilon}_{uz} = \varepsilon_{zu} = \left(\frac{\sqrt{3}}{2}\right)^{n-1} k \tau^n \quad (11)$$

Combinations of these types of loading are of special interest for the evaluation of these constitutive equations. In all cases in which the stress components are parts of the trace of the stress tensor, e. g. under tension load and internal pressure, a combination of these loads lead to a redistribution and to an alteration of the stresses and strain rates.

Superpositions with shear stress components, caused by an additional torque, show no redistribution but only a simultaneous increase of all strain rate components caused by the increase of the deviatoric stress.

As an example, the circumferential strainrate of a tube under constant internal pressure is given by

$$\dot{\varepsilon}_u = \left(\frac{\sqrt{3}}{2}\right)^{\frac{n-1}{2}} k \left(\Delta p \frac{r}{d}\right)^n \quad (12)$$

Under an additional tensile load the three main strain rates show a behaviour as shown in Fig. 3. While the radial and axial strain rates $\dot{\varepsilon}_r$ and $\dot{\varepsilon}_z$ increase, the circumferential strain rate $\dot{\varepsilon}_u$ increases in first stage and decreases at higher axial stresses.

A tube specimen under internal pressure and a superimposed torque show another behaviour of the strain rates. The axial strain rate remains zero and the circumferential strain rate increases directly dependent on the increase of the deviatoric stress. Additionally the shear strain rate $\dot{\varepsilon}_{uz}$ occurs (Fig. 3b).

Furthermore such loading conditions are of interest, in which one portion is a primary loading and another portion is caused by secondary stresses. A combination of constant tensile stress in axial direction and a constant shear strain cause a relaxation of the torsional shear stress, where

- the axial strain rate decreases in the same way as the deviatoric stress decreases
- the relaxation rate of the shear stress increases with an increase of the axial tensile stress.

In Fig. 4a the behaviour of the axial strain rate dependent on time under constant tensile stress and relaxing shear stress is shown. With the time dependent decrease of the shear stress the axial strain rate decreases to the strain rate under unique constant tensile stress. Fig. 4b shows the relaxation behaviour of the shear stress superimposed with different constant tensile stresses.

These theoretical investigations are the basis for the experimental work.

3. Experimental Investigations

3.1 Test programme

The investigations of multiaxial creep on tubes are based on an extended materials evaluation program for HTR components in which a certain number of high temperature creep resistant alloys are subjected to standardised tests /7, 8/. This programme provided the design values. The experimental examination concerning multiaxial creep should help to answer questions related to inelastic analysis and simplified approximations. This results in a test matrix given in Table 2. With the exception of internal pressure all loadings were applied either stationally (stat), cyclically (cycl.) or relaxing (rel). Some of the test combinations were carried out with the same tube specimen in order to avoid the effects of scatter in the materials parameters.

number of tests	internal pressure	tension			torsion		
		stat	cycl	rel	stat	cycl	rel
6	x						
5		x					
12		x	x				
4	x	x					
3	x	x	x				
2	x			x			
2					x		
6					x	x	
3	x				x		
2	x				x	x	
2	x						x
3		x			x		
3		x			x	x	
2		x					x
2		x	x				x
2	x	x			x		

Table 2: Test program to investigate the multiaxial creep behavior

3.2 Experimental Realisation

The experiments for multiaxial creep were performed on typical tubes as used for construction of the prototype heat exchanger and methane steam reformer. The dimensions of the tube specimens are listed in Table 1. The mechanical loadings were applied using servo hydraulic Instron test machines with load capacity of 100 kN for tensile and 500 Nm for torsion for heat exchanger tubes and 500 kN tensile load for reformer tubes. The

tubes were heated by multizone resistance furnaces. The internal pressure was supplied by a gas inlet through the flanges at the ends of the tube specimens and regulated by a pressure valve.

The strains in axial direction were measured by the movement of the piston and calibrated by specific tests. The angle of torsion of the specimen was determined by the twist angle of piston and by calibration tests. A continuous measurement of the radial deformation was not carried out because of the distortion of the continuous temperature profile. The radial deformation was measured after periodical interruptions of the tests.

4. Results and discussion

The numerous test results /9, 10, 11/ of this multiaxial creep programme are now discussed with the main emphasis on torsional creep.

4.1 Constant tensile and torsion loading

At loading the shear strain rate is described by equation 11. The results in Fig. 5 represent the shear creep strain for the shear stresses of 20 MPa and 13.3 MPa at a test temperature of 950 °C The analysis of this curves provide a value of the Norton's exponent n of 5.7; typical values for Alloy 617 obtained in uniaxial creep tests are between 4.5 to 6.5.
Under combined tension and torsion the axial strain rate and the shear strain rate increases in direct proportion to the increase of the v. Mises deviatoric stress

$$\sigma_v = \sqrt{\sigma_z^2 + 3\tau^2} \qquad (13)$$

and the relation ship between tensile and shear stress

$$\beta = \sigma_z / \sqrt{3}\tau \qquad (14)$$

results in an increase of shear strain rate proportional to $(1 + \beta^2)^{\frac{n-1}{2}}$ and an increase of axial strain rate proportional to $(1 + \beta^{-2})^{\frac{n-1}{2}}$.

Fig. 6 illustrates the increase of the axial strain rate dependent on β. The measured points (dots) fit well in the range of values, compared with the calculated curves.

4.2 Relaxing of torsion under constant tension

A constant twist angle on the tube results in the temperature range of creep to a relaxation of the shear stress combined with the constant tensile stress with application of equation the relaxation of the shear stress behaves according to

$$\dot{\tau} = -(3/2)^2 \quad (1 + \beta^2)^{\frac{n-1}{2}} \quad k\, E\, \tau^n \qquad (15)$$

This means with continuing constant tensile stress the relaxation accelerate.
The experimental obtain shear stress relaxation (Fig. 7a) corresponds with an decrease in the axial strain rate (Fig. 7b).

4.3 Superimposed cyclic load

The superimposition of a cyclic stress in axial direction of the form

$$\sigma = \bar{\sigma} + \tilde{\sigma} \sin\omega t \qquad (16)$$

results in a increase of axial strain rate represented by the factor:

$$f^{\dot{\varepsilon}} = 1/t_c \int_{t}^{t+t_c} (1 + \alpha \sin\omega t)^n \, dt \qquad (17)$$

whereby is defined as $\alpha = \tilde{\sigma}/\bar{\sigma}$.
Fig. 8 summarizes the results of a test under tensile pulsation stress combined with relaxing shear stress. On the left hand the relaxation curve of the shear stress once combined with cyclic tensile stress and once combined with constant tensile stress are given. The right hand graph shows the related axial strain behaviour. The postulation of volume constancy requires that under accelerated strain rate, caused by the superimposed cyclic tensile stress, the shear strain rate and the relaxation rate of shear stress decreases.

4.4 Test with load reversals

The calculations of the test were made by application of the v. Mises theory and by Norton's creep law and can describe only multiaxial stationary creep. In order to calculate loading conditions containing changes in load level and inversions of load a consideration of hardening rules is necessary. For the verification of well known rules or to create new rules which fit the component behaviour better, some tests with stepwise chances and inversions of stresses strain rates under different combinations of loadings were carried out.

As an example Fig. 9 shows the torsional shear strain in dependence time for a test with periodical inversions of torque. The calculation based on Norton's creep law without hardening terms results in creep strain after the 2nd. cycle of zero. As a matter of fact the material shows a softening of the torque. After further inversions the amount of softening becomes less and comes to a steady value.

Fig. 10 shows the results of a test with periodical inversion of torque combined with a constant tensile load. As expected the shear strain is higher than in the test before. Meantime the softening increases with each load inversion. The diagram below shows the axial strain of the tube, which is influenced marginally by the behaviour of the shear strain.

5. Final remarks

Multiaxial creep of Alloy 617 tubes can be described mathematically by the v. Mises' theory using the Norton's creep law as the constitutive equation. The theoretically derived formulas for the stress-strain-time behaviour give an acceptable approximation to the obsered deformation behaviour of tubes under multiaxial loading conditions.
Combinations of tension and torsion loadings results depending on the kind of combination,in an acceleration either of the shear stress relaxation or the axial creep strain rate.

Acknowledgment

This investigation was carried out for the German HTGR project PNP under the sponsorship of The Federal Ministry for Science and Technology, The Federal Ministry for Reactor Safety and environment, and The Ministry of Economics, Small Business and Technology of North Rhine Westphalia.

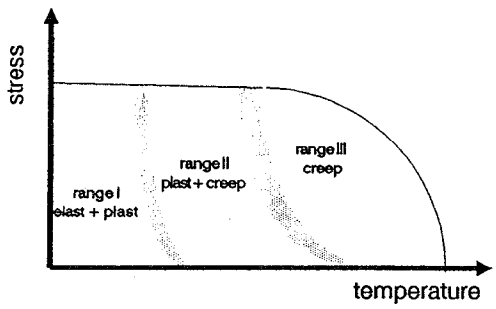

Fig. 1: Bounderies between different behavior of metallic material under mechanical load according to RABOTNOV /2/

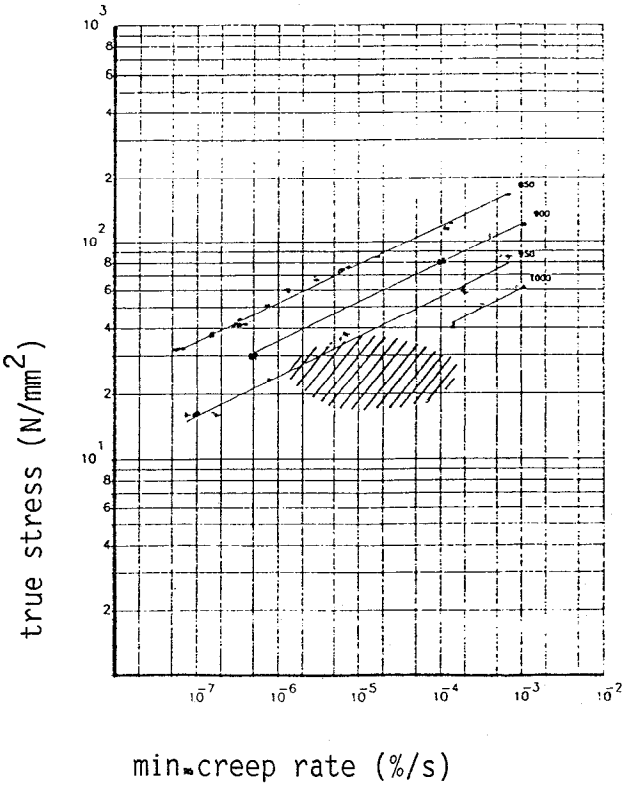

Fig.2: Results of creep rupture tests

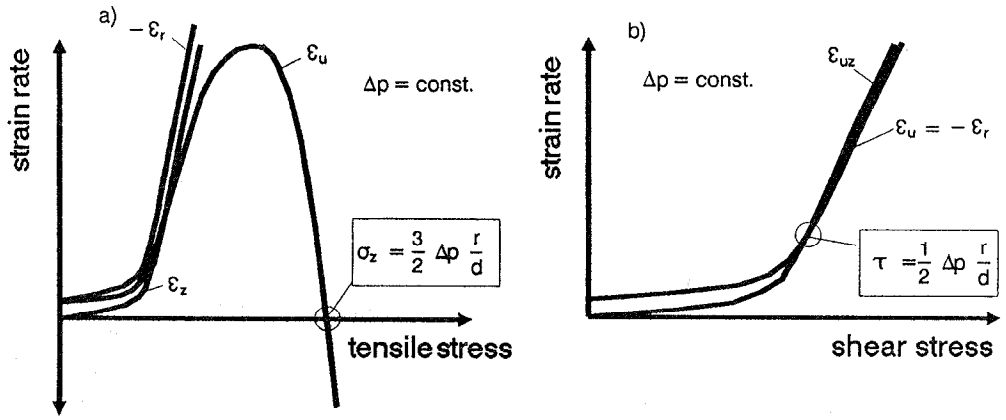

Fig. 3: Redistribution of strain rates under different loading conditions:
- a) internal pressure and additional axial tension
- b) internal pressure and additional torque

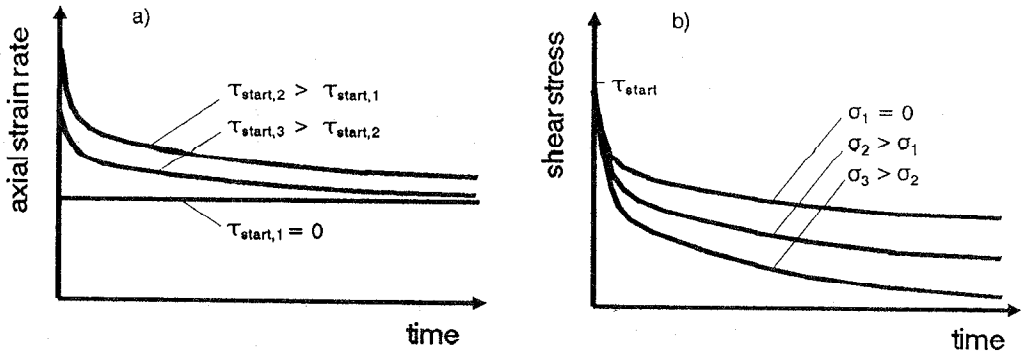

Fig. 4: Interaction betwen the constant tensile stress and a relaxing torsional shear stress:
- a) Influence of the relaxing shear stress on the axial strain rate
- b) Accelleration of the relaxation rate of the shear stress under konstant tensile stress

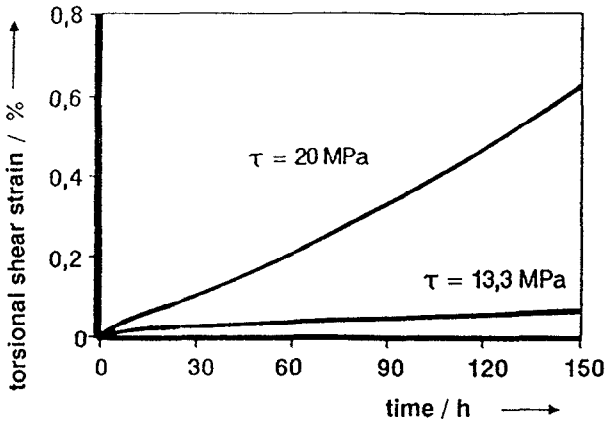

Fig. 5: Creep strain of INCONEL 617 tubes loaded by torsion

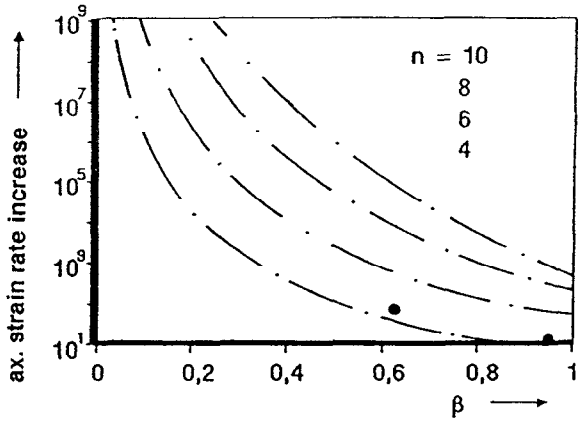

Fig. 6: Increase of the axial strain rate for IHX-tubes under superimposed torsional loading

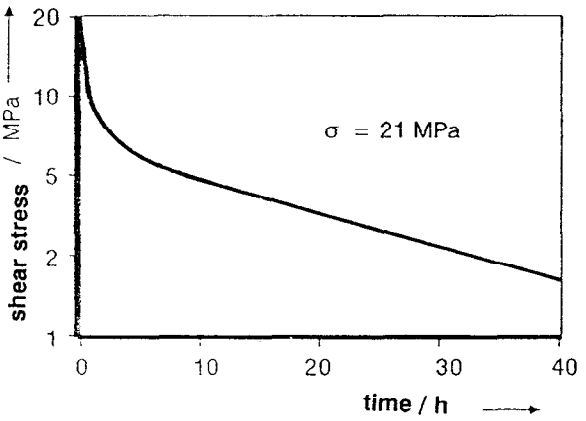

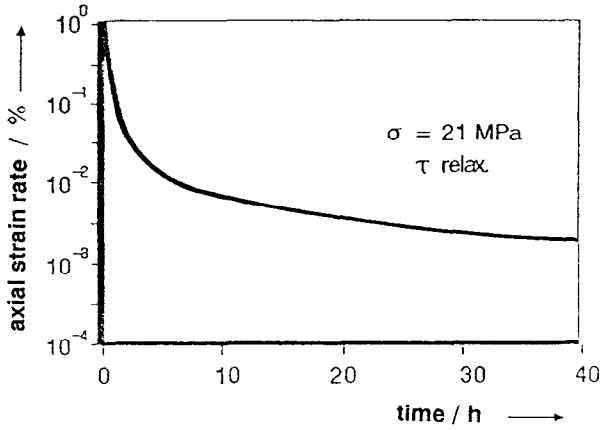

Fig. 7: Relaxing shear stress under superimposed constant axial stress (a) and corresponding axial strain rate (b), INCONEL 617, IHX-tubes

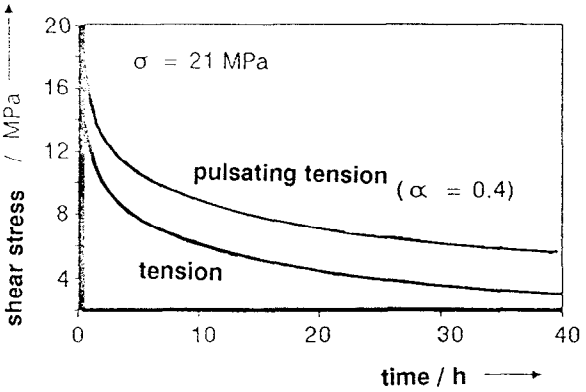

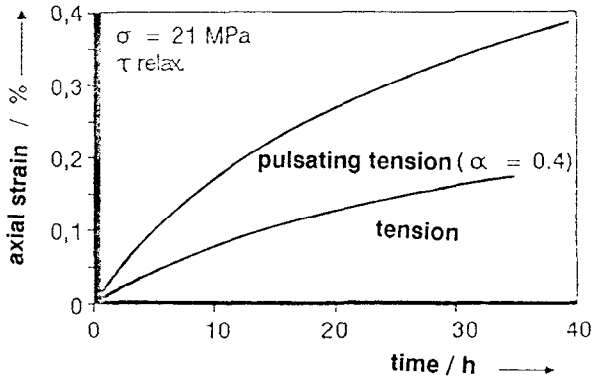

Fig. 8: Relaxing shear stress under superimposed tension and pulsating tension respectively (a) and related strain rate (b), INCONEL 617, IHX-tubes

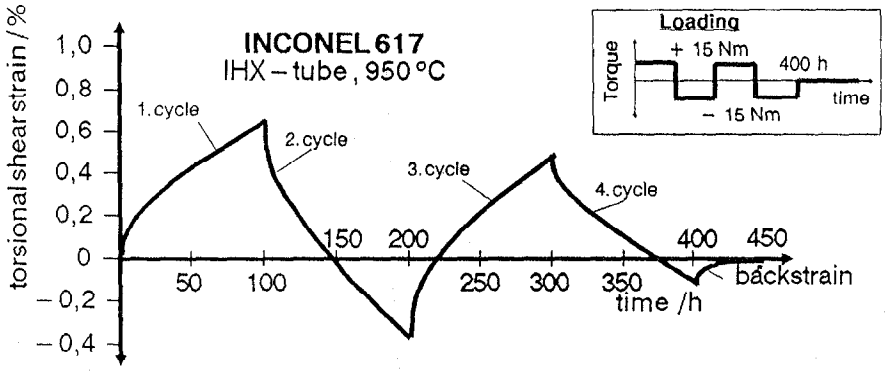

Fig. 9: Torsional shear strain in denpendence on time as result of a test with periodicaly inversed torque

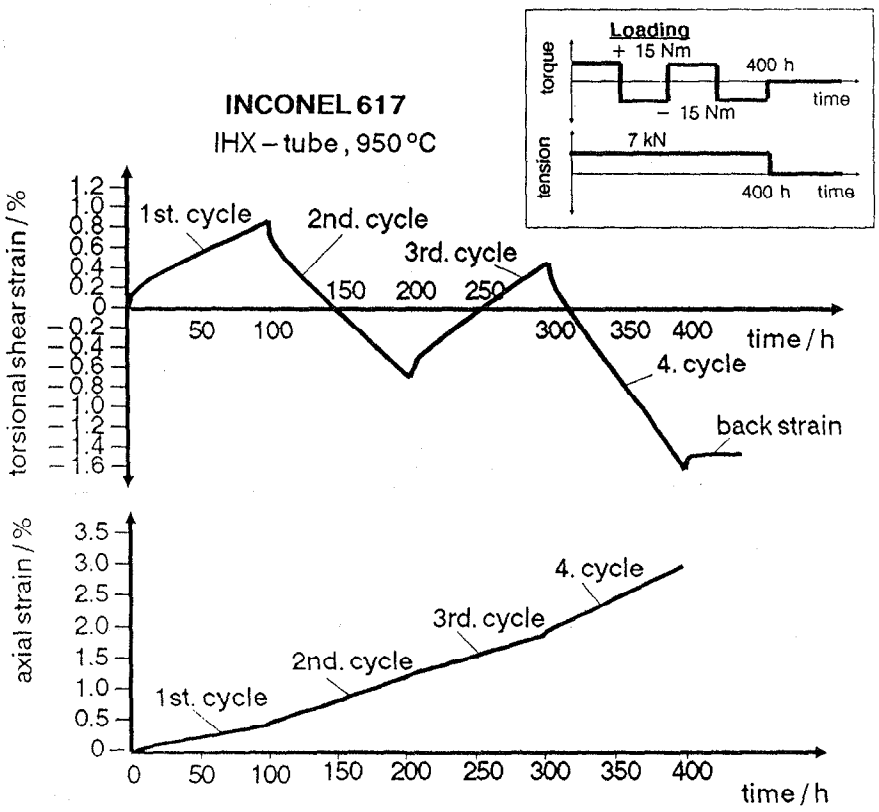

Fig. 10: Torsional shear strain and axial strain in denpendence on time as result of a test with periodicaly inversed inversed torque combined with a constant tensile load.

6. Literature

/1/ R. v. Mises: "Mechanik der festen und flüssigen Körper im plastisch deformablen Zu- stand", Königl. Ges. der Wiss., Göttingen, 1913

/2/ Y. N. Rabotnov: "Creep Problems in Structural Members", North Holland Publishing Com- pany, Amsterdam 1969

/3/ F. H. Norton "Creep of Steels at High Temperature", McGraw Hill, New York, 1929

/4/ K. Franzke, H.-J. Penkalla, M. Rödig, F. Schubert, H. Nickel: "Untersuchungen zum Kriechverhalten von Rohren aus X10NiCrAlTi 32 20 (Nicrofer 32 20) im Anlieferungszustand bei mehrachsiger Belastung", Jül-2127, 1987

/5/ G. Breitbach, S. Kragel, M. Rödig, H.-J. Penkalla: "Zur Berechnung von Kriechverformungen und Spannungen in dickwandigen Rohren", Jül.-Spez. 373, 1986

/6/ F. K. G. Odqvist, J. Hult: "Mathematical Theory of Creep and Creep Rupture", Oxford, 1966

/7/ M. Rödig, H.-J. Penkalla, W. Hannen, H. Hellwig: "Versuche zur komplexen Beanspruchung von Rohrabschnitten bei Tempera- turen oberhalb 800 °C" VDM-Tagung "Werkstoffprüfung 87", Dez. 1987, Bad Nauheim

/8/ H. Nickel, F. Schubert: "Hochtemperaturwerkstoffe für Rohrleitungen in Kernkraftwerken", 3R international 20, 8, 1981, S. 396-404

/9/ H.-J. Penkalla, M. Rödig, M. Hoffmann: "Übertragbarkeit von zeitabhängigen Kennwerten und von Stoffgesetzen auf mehrachsige Belastungsfälle", 10. MPA-Seminar, 1984, Bd. 2

/10/ M. Rödig, H.-J. Penkalla, K. Franzke, F. Schubert, H. Nickel: "Untersuchungen an Rohrproben aus INCOLOY 800 H bei einachsiger und mehrachsiger Beanspruchung", Jül.-Bericht 1975, 1985

/11/ H.-J. Penkalla, F. Schubert, H. Nickel: Kriechverhalten von Rohren aus X10NiCrAlTi 32 20 und NiCr 22 Co 12 Mo unter mehrachsiger statischer und zyklischer Belastung; 13. MPA-Semi- nar, Oktober 1987